

# Overexpression of microRNA-34a Attenuates Proliferation and Induces Apoptosis in Pituitary Adenoma Cells via SOX7

Zijiang Yang,<sup>1,4,5</sup> Ting Zhang,<sup>2,5</sup> Qiping Wang,<sup>3</sup> and Heng Gao<sup>3</sup>

<sup>1</sup>Jiangyin People's Hospital Affiliated to Nantong University, Shoushanlu No. 163, Jiangyin, Wuxi 214400, China; <sup>2</sup>Central Laboratory, Jiangyin People's Hospital Affiliated to Nantong University, Shoushanlu No. 163, Jiangyin, Wuxi 214400, China; <sup>3</sup>Neurosurgery, Jiangyin People's Hospital Affiliated to Nantong University, Shoushanlu No. 163, Jiangyin, Wuxi 214400, China; <sup>4</sup>Neurosurgery, The First People's Hospital of Kunshan, Qianjinxilu No. 91, Kunshan, Suzhou 215300, China

**Pituitary adenomas constitute one of the most common intracranial tumors and are typically benign. However, the role of the tumor suppressor microRNA-34a (miR-34a), which is implicated in other cancers, in pituitary adenoma pathogenesis remains largely unknown. miR-34a expression was compared between GH4C1 cancer cells and normal cells derived from the pituitary gland of *Rattus norvegicus*, and the effects of miR-34a on GH4C1 cell proliferation and apoptosis were examined. miR-34a target genes were identified and analyzed computationally. The mRNA levels of the miR-34a target genes were measured using qRT-PCR, and the protein levels of the differentially expressed targets were assessed by western blotting. miR-34a expression was significantly lower in GH4C1 cells, whereas miR-34a overexpression significantly inhibited GH4C1 cell proliferation and promoted cell apoptosis through SRY-box 7 (SOX7). Our data facilitate the development of a better understanding of the pathogenesis and treatment of pituitary adenomas by elucidating the crucial role of miR-34a in the development of pituitary adenomas.**

## INTRODUCTION

Pituitary adenomas constitute the most common intracranial tumors after gliomas and meningiomas, accounting for approximately 22.5% of cases.<sup>1</sup> Most pituitary adenomas are benign and are rarely malignant, with only 0.1%–0.2% of cases progressing to pituitary carcinoma.<sup>2</sup> Conversely, the associated dysregulation of hormone secretion and occupation of intracranial space may cause serious morbidity, which is often compounded by typically late diagnosis and lack of effective treatments for recurrent cases. The etiology of pituitary adenoma remains unclear, although surveys in recent decades have identified possible diagnostic and therapeutic biomarkers. However, these surveys were limited by small sample size, lack of normal human pituitary tissues as controls, and the absence of rigorous high-throughput studies. Hence, elucidation of the molecular pathogenesis of pituitary adenomas and identification of reliable diagnostic and therapeutic biomarkers remain critical.

Pituitary adenomas are classified based on residual hormone secretion. In China,<sup>3</sup> 42.70% of cases show no hormone secretion, whereas

24.50%, 10.20%, 9.00%, and 2.10% show prolactin, growth hormone, follicle-stimulating hormone, and adrenocorticotrophic hormone secretion, respectively. All other cases are characterized by the secretion of multiple hormones, including luteinizing hormone and thyroid-stimulating hormone. The molecular mechanisms underlying different types of adenomas may vary; therefore, for example, the GH4C1 rat pituitary cell line is suggested as a model of growth hormone-secreting adenomas. Furthermore, depending on whether the tumor diameter is more or less than 10 mm, 45.5% and 54.5% of cases are classified as macro- and microadenomas, respectively,<sup>3</sup> of which the latter are more likely to be aggressive.

Although genes such as vascular endothelial growth factor precursor<sup>4</sup> and cyclin D<sup>5</sup> have been demonstrated both *in vitro* and *in vivo* to regulate proliferation, invasion, and apoptosis in pituitary adenomas and GH4C1 cells, several other genes may also be involved. In general, the development of many cancers is driven by specific genes. For example, *MYC* is a well-established oncogene that promotes cell growth, proliferation, and malignant transformation.<sup>6</sup> *BCL-2* and *BAX*<sup>7,8</sup> are also associated with cancer development. Similarly, high-mobility group box 1 protein (HMGB1) and interleukin (IL)-16 have been shown to play dual roles in cancer development.<sup>9,10</sup> *SOX7*, a member of the F group of SOX proteins that contains a high-mobility group DNA-binding domain, was also recently demonstrated to inhibit tumorigenesis.<sup>11</sup>

MicroRNAs are short noncoding RNAs of 18–25 nt that bind to the 3' UTR of target mRNAs to suppress translation or promote posttranscriptional mRNA cleavage, depending on the degree of sequence complementarity.<sup>12</sup> Conversely, microRNAs may activate translation by binding to the 5' UTR of the target gene or to the protein itself.<sup>12</sup> Finally, microRNAs may also directly bind or modulate methylation

Received 12 September 2017; accepted 5 July 2018;  
<https://doi.org/10.1016/j.omto.2018.07.001>.

<sup>5</sup>These authors contributed equally to this work.

**Correspondence:** Heng Gao, PhD, Jiangyin People's Hospital Affiliated to Nantong University, Shoushanlu No. 163, Jiangyin, Wuxi 214400, China.

**E-mail:** [drgaoheng1971@126.com](mailto:drgaoheng1971@126.com)



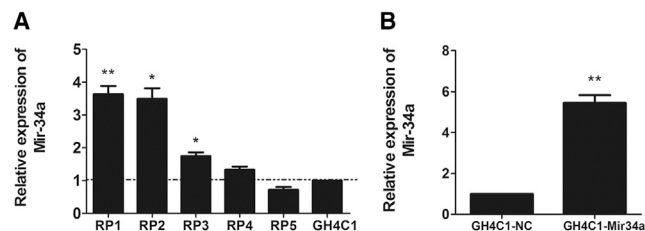


**Figure 1. miR-34a Different Expression**

*miR-34a* expression in GH4C1 cells before and after transfection. (A) *miR-34a* expression was measured by qRT-PCR in GH4C1 cells and normal rat pituitary tissues, using U6 as an internal control. (B) *miR-34a* expression was also assessed by qRT-PCR after transfection with *miR-34a* mimic oligos. \* $p < 0.05$ ; \*\* $p < 0.01$ .

at the promoter of target genes.<sup>13</sup> In the past decade, an increasing number of microRNAs have been demonstrated to regulate the development and progression of pituitary adenomas, including let-7, miR-15a, miR-16-1, miR-26b, miR-122, miR-128, and miR-493.<sup>14–17</sup> *miR-34a* is a well-established tumor suppressor that is widely implicated in many tumors and inhibits cancer cell proliferation, invasion, and metastasis by targeting platelet-derived growth factor receptor beta, mesenchymal-epithelial transition (MET) proto-oncogene, and transforming growth factor beta receptor 2.<sup>18,19</sup> However, its role in pituitary adenomas remains unknown. The aim of the present study was, therefore, to investigate the role of this microRNA (miRNA) in pituitary adenomas, using GH4C1 cells as a model system. Moreover, the relationship between *miR-34a* and *Sox7*, *Bcl2*, *Bax*, *Myc*, *Hmgb1*, and *Il16* was additionally investigated, as this is yet undefined in pituitary adenomas.

## RESULTS

### *miR-34a* Is Downregulated in Pituitary Adenoma Cells

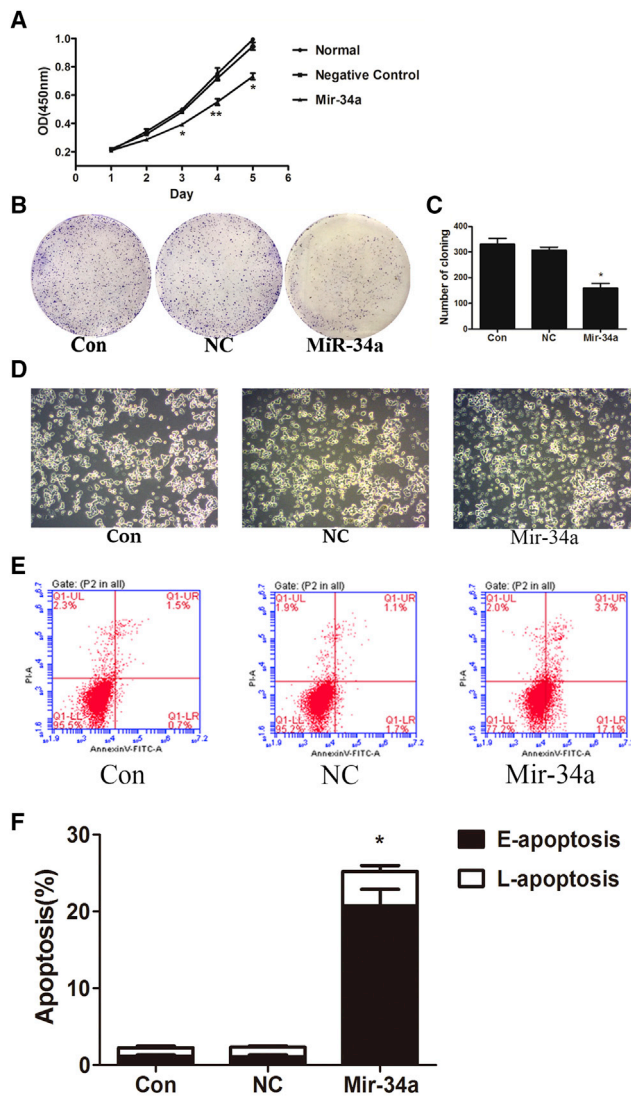
*miR-34a* expression was more than 3- to 4-fold lower in GH4C1 cells than in normal rat pituitary tissue ( $p < 0.05$ ; Figure 1A). To determine the specific functions of *miR-34a* in pituitary adenomas, we transfected GH4C1 cells with a *miR-34a* mimic to obtain a cell line with 5-fold higher *miR-34a* levels than cells transfected with the negative control ( $p < 0.05$ ; Figure 1B).

### *miR-34a* Overexpression Inhibits Proliferation

To determine whether *miR-34a* exerted anti-proliferative effects, cell proliferation was measured after 1–6 days in mimic-, negative control oligonucleotide-transfected, and GH4C1 cells. Microscopy showed that high *miR-34a* levels significantly suppressed cell proliferation (Figures 2A and 2D). Moreover, a colony-formation assay revealed that clonogenic survival was obviously decreased following increase in *miR-34a* levels (Figures 2B and 2C;  $p < 0.05$ ).

### *miR-34a* Overexpression Induces Apoptosis

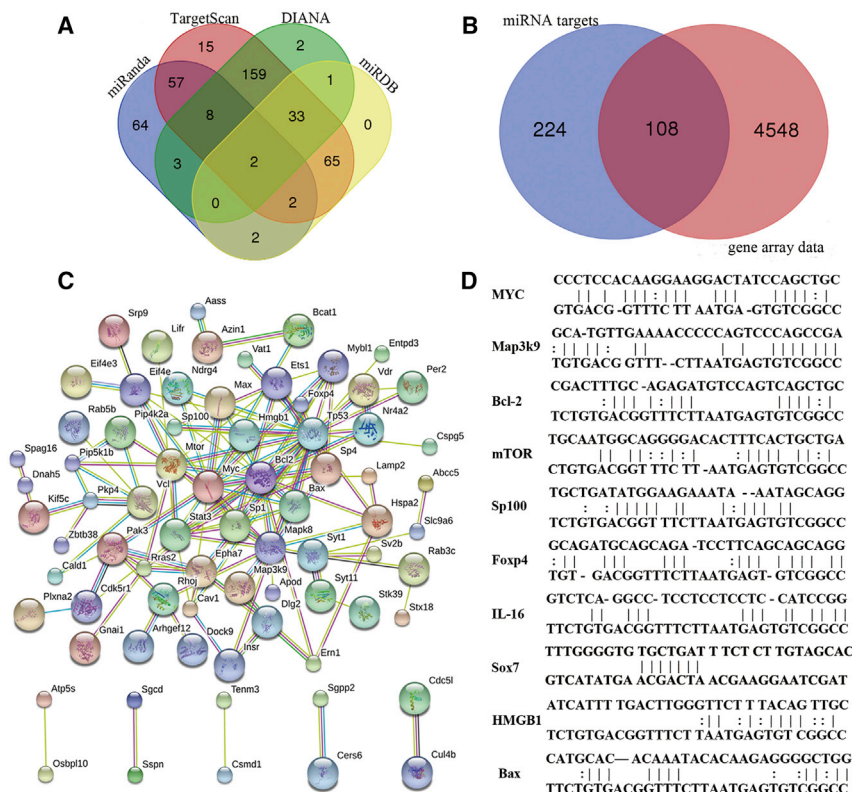
Apoptosis was measured by flow cytometry in cells transfected with the *miR-34a* mimic or the negative or blank GH4C1 cell controls. In the resulting plots (Figures 2E and 2F), cells clustered in the lower right quadrant are in early apoptosis. In contrast, late apoptotic and necrotic cells are located in the upper right quadrant, and cells in



**Figure 2. Effect of *miR-34a* on Cell Proliferation and Apoptosis**

Effects of *miR-34a* on proliferation and apoptosis in GH4C1 cells. (A) Proliferation was assessed using the Cell Counting Kit-8 at 1–6 days after transfection with the *miR-34a* mimic, negative control, and blank GH4C1 cell controls. (B) Colony-formation assay after transfection with the *miR-34a* mimic, negative control, or blank GH4C1 cell controls. (C) Statistical analysis of results of the colony-formation assay after transfection with the *miR-34a* mimic, negative control, or blank GH4C1 cell controls. (D) Effects of *miR-34a* on proliferation 5 days after transfection. Original magnification: 40 $\times$ . (E and F) In (E), apoptosis was assessed by annexin V-FITC and propidium iodide staining and flow cytometry after transfection with the *miR-34a* mimic, negative control, and blank GH4C1 cell controls. (F) Statistical analysis of the apoptosis index after transfection with the *miR-34a* mimic or negative control. Con, blank control group; E, early; L, late. \* $p < 0.05$ ; \*\* $p < 0.01$ .

the last stage of apoptosis cluster are located in the upper left quadrant. The proportions of cells in early, late, and final stages of apoptosis were 1.7%, 1.1%, and 1.9%, respectively, in GH4C1 cells transfected with the negative control; the percentages were 0.7%, 1.5%, and 2.3%, respectively, in blank control cells and 17.1%, 3.1%,

**Figure 3. Target Gene Identification**

Candidate target genes and functional enrichment. (A) Venn diagrams showing the intersection of candidate target genes identified in four microRNA databases. (B) Venn diagrams showing the intersection between target genes identified in microRNA databases and in two sets of gene array data. (C) Protein-protein interactions among miR-34a target genes, with interaction scores set to medium confidence (0.400) and disconnected nodes hidden. Pink indicates experimentally determined known interactions; blue indicates known interactions from curated databases; yellow indicates text mining; green indicates predicted interactions by gene neighborhood; black indicates co-expression. (D) Sequence complementarity in RNA22.

Most of the top 15 KEGG pathways are implicated in cancer development (summarized in Table S5). In contrast, transcriptional regulation was significantly enriched in the top five enriched GO terms “molecular function,” “biological process,” and “cellular component” (summarized in Table S5). Based on protein-protein interactions (Figure 3C) and sequence complementarity measured in RNA 22 (Figure 3D), *Myc*, *Bcl2*, *Sp100*, *Sox7*, *Hmgb1*, *Mtor*, *Map3k9*, *Foxp4*,

and 2.0%, respectively, in blank control cells transfected with miR-34a (Figure 2E). The proportion of cells in early apoptosis and in late apoptosis in the miR-34a mimic group was significantly higher than that in the negative control group and in the blank control (Figure 2F;  $p < 0.05$ ). These results indicate that miR-34a elicits apoptosis in GH4C1 cells.

#### miR-34a Target Genes and Functional Enrichment

miR-34a target genes in GH4C1 cells were predicted with high stringency based on four miRNA databases and two sets of gene array data. Briefly, 3,409 candidate target genes were collected from the miRanda, TargetScan, miRDB, and DIANA databases (the targets from the four databases are summarized in Table S1) and filtered in Excel to identify genes repeated at least twice in different databases. For 413 genes, candidates that appeared twice in the same database were also retained, of which, 332 were present in at least two databases (Figure 3A; summarized in Table S2). In contrast, the gene arrays GEO: GSE2175 and GSE4237 in gnen cloud of biotechnology information (GCBI) indicated that 4,656 mRNAs were significantly dysregulated by at least 2-fold ( $p < 0.05$ ) in pituitary adenomas (summarized in Table S3). A Venn diagram (Figure 3B) for dysregulated mRNAs from the array data and target genes in miRNA databases identified 108 candidates for further analysis (summarized in Table S4).

Enrichment analyses with ONTO-TOOLS and GOEAST GO indicated that 54 Kyoto Encyclopedia of Genes and Genomes (KEGG) pathways and 446 GO processes were enriched in the 108 candidates.

*Il16*, and *Bax* were selected for further analysis by qRT-PCR. MYC, BAX, BCL-2, HMGB1, SOX7, and IL-16 were also selected for validation by western blot.

#### Validation of miR-34a Target Genes

Western blotting demonstrated that GH4C1 cell transfection with the miR-34a mimic significantly suppressed MYC, BCL-2, HMGB1, and SOX7 expression, even as BAX and IL-16 accumulated (Figure 4A). Furthermore, experimental validation of the miR-34a targets, BCL-2, MYC, and SOX7, using a luciferase reporter system was performed (Figure 4B). Luciferase reporter assays showed that miR-34a reduced the luciferase activity of the *Sox7* 3' UTR but not that of *Bcl2* and *Myc*. However, mutated *Sox7* alleviated the inhibitory effect of miR-34a on the luciferase activity (Figures 4C and 4D). These results suggested that miR-34a directly regulates *Sox7* mRNA expression.

#### SOX7 Downregulation Suppresses Proliferation and Induces Apoptosis

To determine whether the regulation of SOX7 expression by miR-34a plays an important role in cell proliferation and apoptosis, three SOX7 small interfering RNAs (siRNAs) were constructed. Small interfering (Si)-SOX7 #2 and #3 sequence significantly inhibited SOX7 expression at the mRNA and protein levels in GH4C1 cells, as determined by qRT-PCR and western blotting, using beta-actin and GAPDH as controls (Figures 5A and 5B). Furthermore, we found that SOX7 knockdown restrained cell proliferation, as assessed using

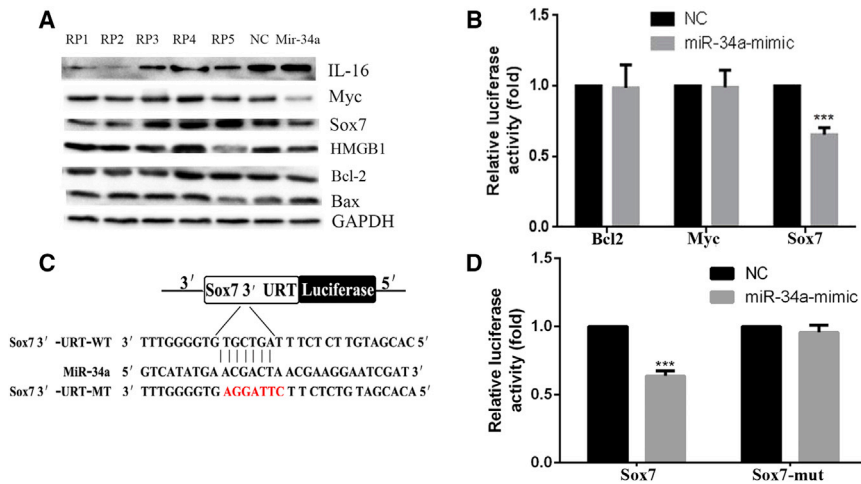


**Figure 4. Sox7 Dual-Luciferase Reporter**

miR-34a targets the *Sox7* gene in GH4C1 cells. (A) Target gene protein levels visualized by western blotting.

(B) Luciferase reporter validation of whether miR-34a could directly bind on *Bcl2*, *Myc*, or *Sox7* mRNA in GH4C1 cells. (C) Schematic representation of the *Sox7* 3'UTR showing putative miRNA target sites; sequence in red indicates mutated potential miR-34a binding sites. (D) GH4C1 cells were co-transfected with a luciferase reporter containing the *Sox7* 3' UTR and miRNA mimics in parallel with mutated *Sox7*. At 48 hr after transfection, the luciferase intensity was measured. \*\*\**p* < 0.01.

Cell Counting Kit-8 (CCK-8) at 1–5 days and microscopic observation at 4 days after SOX7 knockdown (Figures 5C and 5D). Knockdown of SOX7 yielded much higher apoptosis rates than that observed in the control group. The proportions of cells in the early, late, and final stages of apoptosis were 1.2%, 0.9%, and 2.3%, respectively, in GH4C1 cells transfected with the negative control; however, the percentages were 16.4%, 6.6%, and 4.5%, respectively, in siRNA-SOX7 #2 cells; and 23.5%, 7.3%, and 2.2%, respectively, in siRNA-SOX7 #3 cells (Figure 5E). The proportion of cells in early and late apoptosis in siRNA-SOX7 #2 and in siRNA-SOX7 #3 was significantly higher than that in the negative control group (Figure 5F; *p* < 0.05). These results indicated that SOX7 inhibits apoptosis in GH4C1 cells.

## DISCUSSION

miR-34a suppresses many forms of cancer, and several studies have shown that it is downregulated in cancers such as glioma,<sup>20</sup> breast cancer,<sup>21</sup> and bladder carcinoma.<sup>22</sup> In particular, miR-34a elicits a range of biological effects by directly or indirectly regulating the expression of genes crucial for differentiation (sirtuin 1; *SIRT1*),<sup>23</sup> proliferation and apoptosis (*TGFBR2*),<sup>19</sup> cell-cycle progression (*CD44*),<sup>22</sup> invasion and metastasis (tumor protein D52),<sup>21</sup> protein phosphorylation (*VEGF*),<sup>24</sup> angiogenesis (*CD44*),<sup>25</sup> epithelial-mesenchymal transition (sterile alpha motif domain-containing 3),<sup>26</sup> autophagy (*HMGB1*),<sup>27</sup> and chemosensitivity (AXL receptor tyrosine kinase).<sup>28</sup> Notably, this miRNA is encoded in chromosome 1p36, which is strongly regulated by p53.<sup>29</sup> Yamakuchi et al.<sup>30</sup> described a positive-feedback loop, in which p53 induces miR-34a, which, in turn, suppresses *SIRT1* to stimulate p53 activity. However, whether the p53-miR-34a positive-feedback loop actually exists in pituitary adenomas requires further investigation.

Herein, we report that *Sox7*, *Myc*, *Bcl2*, *Bax*, *Hmgb1*, and *Il16* were predicted to contain potential miR-34a binding sites. In addition to the *Myc* oncogene,<sup>6</sup> the HMGB1 transcription factor, and the pleiotropic immune response factor IL-16,<sup>9,10</sup> dysregulation of anti-apoptotic proteins such as BCL-2 and pro-apoptotic proteins such

as *Bax*<sup>7</sup> is also associated with cancer development. Paradoxically, both BCL-2 and BAX are simultaneously expressed in some cancers.<sup>8</sup> In turn, SOX7 inhibits tumorigenesis.<sup>11</sup> We subjectively chose three of the target genes for luciferase reporter validation experiments, which demonstrated miR-34a directly binding on the *Sox7* 3' UTR. Our findings demonstrate, for the first time, that miR-34a suppresses pituitary adenomas by directly downregulating *Sox7*. We observed that, similar to pituitary adenomas, miR-34a is less abundantly expressed in GH4C1 cells than in normal rat pituitary tissue and that miR-34a overexpression inhibits cell proliferation. miR-34a also stimulates apoptosis, which corroborates previous observations in non-small-cell lung cancer.<sup>19</sup>

SOX7 constitutes a key molecule associated with tumorigenesis,<sup>11</sup> although the underlying mechanisms are unclear. For example, SOX7 was demonstrated to suppress lung<sup>31</sup> and breast cancer.<sup>32</sup> Recently, Cuvertino et al.<sup>33</sup> showed that, in contrast to the conventional view, SOX7 is an oncogene that promotes the proliferation of acute lymphoblastic cells. Katoh<sup>34</sup> reported that SOX7 expression was upregulated in pancreatic cancer cell lines and in some gastric and esophageal cancer cell lines. In addition, a study demonstrated that overexpression of *Sox7* induced embryonal carcinoma cell differentiation by regulating Gata-4 and Gata-6 expression.<sup>35</sup> SOX7 promotes glioma cell growth by increasing vascular endothelial growth factor receptor 2 (VEGFR2)-mediated vascular abnormality, with high SOX7 expression levels correlating with poor survival, early recurrence, and impaired vascular function.<sup>36</sup> However, Yang et al.<sup>37</sup> reported that SOX7 overexpression induces IL-33 expression to promote metastasis of tumor-associated macrophages. These results suggest that SOX7 does not necessarily play the same role in all cancers. Indeed, the role of SOX7 in pituitary adenomas is unknown, although we found that miR-34a overexpression directly suppressed SOX7 expression at both the mRNA and protein levels, which, in turn, restrained GH4C1 cell proliferation and induced apoptosis. In summary, we report that miR-34a was suppressed in GH4C1 cells. Moreover, we demonstrated that miR-34a inhibits proliferation and induces apoptosis in GH4C1 cells by directly regulating SOX7 levels. SOX7 plays an oncogene role in pituitary adenomas. Nonetheless, collectively, the data suggest that miR-34a plays a crucial

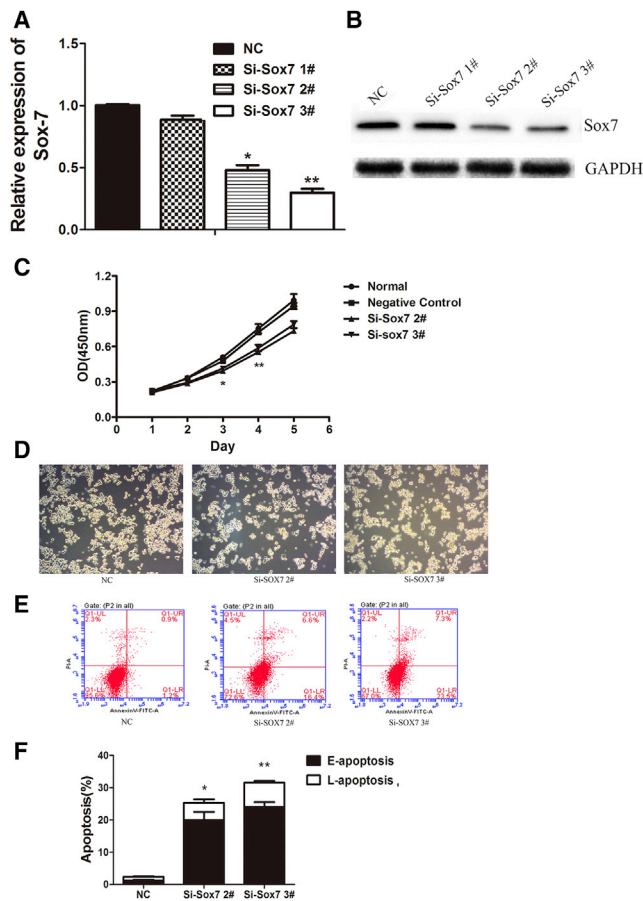


**Figure 5. Effect of Sox7 on Cell Proliferation and Apoptosis**

Effects of SOX7 expression on proliferation and apoptosis in GH4C1 cells. (A and B) Knockdown of SOX7 with different SOX7 siRNA sequences showed that si-SOX7 #2 and #3 significantly inhibited SOX7 expression at the mRNA and protein levels in GH4C1 cells. Beta-actin and GAPDH were used as controls. (C and D) Proliferation was assessed using CCK-8 at 1–5 days after knockdown with siRNAs, negative control, and blank GH4C1 cell controls. Effects of siRNAs on proliferation at 4 days after SOX7 knockdown are indicated. Original magnification: 40 $\times$ . (E) Apoptosis of GH4C1 cells transfected with SOX7 siRNAs and negative control was tested by annexin V-FITC and propidium iodide staining and flow cytometry. (F) Statistical analysis of the apoptosis index after transfection with SOX7 siRNAs or negative control. E, early; L, late. OD, optical density. \* $p < 0.05$ ; \*\* $p < 0.01$ .

role in the development of pituitary adenomas and that targeting of miR-34a activity may provide new opportunities for treatment.

## MATERIALS AND METHODS

### Tissue Collection and Cell Culture

Owing to the lack of normal human pituitary tissue for use as negative control, the pituitary glands were collected from 10-week-old healthy female *Rattus norvegicus* after euthanization with 5% chloral hydrate on ice and washed in PBS (pH 7.2). Procedures involving animals and their care were conducted in conformity with NIH guidelines (NIH Pub. No. 85-23, revised 1996) and were approved by the Animal

Care and Use Committee of the Medical School of Nantong University.

The rat pituitary adenoma cell line GH4C1 was purchased from the American Type Culture Collection (ATCC; Manassas, VA, USA) and cultured in Ham's F10 medium (12390-035, GIBCO, Life Technologies, Gaithersburg, MD, USA) supplemented with 10% fetal bovine serum (10099-141, GIBCO, Life Technologies) at 37°C in an incubator with 5% CO<sub>2</sub> and 95% air.

### RNA Isolation and Real-Time qRT-PCR

Total RNA was extracted from tissues and cells using TRIzol (15596026, Life Technologies), following the manufacturer's instructions. miR-34a was reverse-transcribed and quantified with stem-loop primers, using U6 as an internal control. Target gene expression was quantified using qRT-PCR on a CFX96 real-time system (785BR10081, Bio-Rad, Hercules, CA, USA) using the SYBR Green PCR master mix (RR820A, TaKaRa, Shiga, Japan) and normalized to *Gapdh* expression. Fold change was calculated according to the 2<sup>- $\Delta\Delta$ Ct</sup> method. qRT-PCR primers are listed in Table 1, and miR-34a mimic and negative control oligos are shown in Table 2.

### Transfection

GH4C1 cells (2.0  $\times$  10<sup>5</sup>) were plated in a 6-well dish and allowed to adhere overnight. Cells were transfected with a 5- or 10-nM equimolar mix of miR-34a mimic (GenePharma, Shanghai, China) or negative control oligos (GenePharma) (2 oligos per category) using Lipofectamine 2000 (Invitrogen) and opti-modified Eagle medium (MEM) (Invitrogen, Carlsbad, CA, USA), according to the manufacturer's instructions. Transfection efficiency was assessed by fluorescence microscopy and confirmed by qRT-PCR 48 hr after transfection. The same methods were used to knock down SOX7. Cells (2.0  $\times$  10<sup>5</sup>) were plated into a 6-well dish and allowed to adhere overnight. Cells were then transfected with 3 siRNAs designed against SOX7 combined in an equimolar ratio (20 or 40 nM; SOX7-Rat-1, SOX7-Rat-2, and SOX7-Rat-3, Invitrogen-Thermo Fisher Scientific, Waltham, MA, USA) or a negative control siRNA (Invitrogen-Thermo Fisher Scientific). Transfection efficiency was monitored via fluorescence microscopy and confirmed using qRT-PCR 48 hr after transfection. siRNA transfections were performed in GH4C1 cell lines and utilized in proliferation and apoptosis assays. siRNA-SOX7 and negative control sequence are listed in Table 3.

### Western Blot

Western blotting was used to assess MYC, BAX, BCL-2, HMGB1, SOX7, and IL-16 levels in GH4C1 cells 48 hr after transfection with miRNA oligos. Briefly, equal amounts of protein (40  $\mu$ g) were separated by 12% SDS-PAGE, transferred to polyvinylidene fluoride membranes (Millipore, Bedford, MA, USA), and then blocked in 5% milk in Tris-buffered saline (TBS)-Tween 20 (0.5%). Proteins were then probed with rabbit antibodies against human MYC, BCL2, SOX7, HMGB1, BAX, AND IL-16 (Cell Signaling Technology, Danvers, MA, USA) and corresponding peroxidase-conjugated secondary antibodies (Cell Signaling Technology) and visualized using

**Table 1. Primers for qRT-PCR**

Target	Primers (5'-3')
GAPDH	B661204 (Sangon, Shanghai, China)
mir-34a RT	GTCTGATCCAGTGCAGGGTCCGAGGTA TTCCGACTGGATACGACACAACC
mir-34a-F	GCGGCGGTGGCAGTGTCTTAGC
mir-34a-R	ATCCAGTGCAGGGTCCGAGG
U6 RT	AACGCTTCACGAATTTGCGTG
U6-F	GCTCGCTTCGGCAGCAC
U6-R	GAGGTATTGACACCAGAGGA
MYC-F	CATCAGCACAACACTACGACGC
MYC-R	GCTGGTGCATTTTCGGTTGT
Map3k9-R	AAGCAGAGGTTGGGTTCCCTT
Map3k9-F	GAGGACATCAGCCAGACCAT
Bcl-2-R	ACAGCCAGGAGAAATCAAACA
Bcl-2-F	GGTGACAACATCGCTCTG
Bax-R	AAGCAGAGGTTGGGTTCCCTT
Bax-F	GAGGACATCAGCCAGACCAT
mTOR-R	TTGTGCTCTGGATTGAGGTG
mTOR-F	GGAATGCTGGTGCCTTTGT
Foxp4-R	CGGATAAGGAGGCATAGGT
Foxp4-F	GCAGGAGAAGCAACGACAA
IL-16-R	GACAGGTGGCTGCATAGTGA
IL-16-F	CTGGCCTAACACACCAGGAT
HMGB1-R	GCAGCAGTGTGTGCCACAT
HMGB1-F	CGGCCTTCTTGTGTCTGT
SOX7-R	GCCAAGGGCCAAAGAACCTA
SOX7-F	GGACACATATCCCTACGGGC
SP100-R	GTGTGGGAGGTTGTCTGGAA
SP100-F	GACCAAGCAAGGACTAACGA

enhanced chemiluminescence (ECL) solution (Santa Cruz Biotechnology, Dallas, TX, USA). For Cell Signaling Technology c-MYC (#13987), BAX (#2772), HMGB1 (#6893), and GAPDH (#2118), and for Abcam BCL-2 (ab196495), SOX7 (ab89954), and IL-16 (ab180792), the dilution ratio was 1:1,000.

#### Cell Proliferation and Colony-Formation Assay

GH4C1 cells were seeded in 96-well microplates at 5,000 cells per well and allowed to adhere and grow for 2, 4, 6, 8, and 10 days after transfection. Proliferation was measured at each time point using the CCK-8 (Dojindo, Kumamoto, Japan), following the manufacturer's instructions. Each assay was repeated six times, and the results were averaged. To assess colony formation, cells were seeded in 6-well plates at 2,000 cells per well and transfected with the miR-34a mimic and the negative control. After 1 week, the colonies were fixed with 4% paraformaldehyde and stained with crystal violet (Sigma, St. Louis, MO, USA). Data were collected from three replicates.

**Table 2. miR-34a Mimic and Negative Control Oligos**

Oligo	Sequence
mir-34a (RAT)	5'-UGGCAGUGUCUUAGCUGGUUGU-3' 5'-AACCAGCUAAGACACUGCCAUU-3'
Negative control	5'-UUCUCCGAACGUGUCACGTT-3' 5'-ACGUGACACGUUCGGAGAATT-3'

#### Cell Apoptosis

Apoptosis was measured by annexin V-FITC (fluorescein isothiocyanate) and propidium iodide staining (BD PharMingen, San Jose, CA, USA), according to the manufacturer's instructions. Briefly, GH4C1 cells were collected 48 hr after transfection and resuspended in 100  $\mu$ L of 1 $\times$  binding buffer supplemented with 5  $\mu$ L annexin V-FITC, followed by incubation at room temperature for 15 min in the dark and mixing with 5  $\mu$ L propidium iodide 5 min before analysis. Samples were then diluted with 400  $\mu$ L binding buffer and analyzed by flow cytometry (BD LSRFortessa, Bedford, MA, USA).

#### miRNA Target Prediction

Putative miR-34a targets were identified using miRanda, TargetScan ([http://www.targetscan.org/vert\\_71/](http://www.targetscan.org/vert_71/)), miRDB (<http://mirdb.org/miRDB/index.html>), and DIANA ([http://diana.imis.athena-innovation.gr/DianaTools/index.php?r=microT\\_CDS/index](http://diana.imis.athena-innovation.gr/DianaTools/index.php?r=microT_CDS/index)). RNA22 v2.0 (<https://cm.jefferson.edu/rna22/>) was then used to test sequence complementarity between miR34a and candidate target genes. Consensus targets were defined as genes appearing at least twice in different databases, with  $p < 0.1$  for sequence complementarity against miR-34a.

GCBI (<https://www.gcbi.com.cn/gclib/html/index>) was also mined for genes significantly dysregulated in human pituitary adenomas, using "neoplasm, pituitary," "neoplasms, pituitary," "pituitary neoplasm," "pituitary tumors," "pituitary tumor," "tumor, pituitary," "tumors, pituitary," "pituitary adenoma," "adenoma, pituitary," "adenomas, pituitary," or "pituitary adenomas" as simple search terms. Array data were analyzed to compare mRNA expression between pituitary adenomas and normal pituitary tissue, between invasive and non-invasive pituitary adenomas, and between recurrent and nonrecurrent pituitary adenomas. Array data from gene mutants, stem cells, and transgenic systems were excluded. Finally, the array datasets GEO: GSE2175 and GSE4237 were selected for further analysis.

#### Enrichment Analysis

Enrichment for KEGG pathways and Gene Ontology (GO) terms was assessed using ONTO-TOOLS and GOEAST ([http://omicslab.genetics.ac.cn/GOEAST/php/batch\\_genes.php](http://omicslab.genetics.ac.cn/GOEAST/php/batch_genes.php)), respectively. Protein-protein interactions among miR-34a target genes were reconstructed in String (<https://string-db.org/cgi/input.pl>). Targets were selected for validation by qRT-PCR and western blot.

#### Dual-Luciferase Reporter Assay

For dual-luciferase assays, the *Sox7* 3' UTR containing predicted miR-34a seed-matching sites (wild-type; WT) and corresponding

**Table 3. siRNA-SOX7 and Negative Control Sequence**

	Sequence
Negative control	5'-UUC UCC GAA CGU GUC ACG UTT-3'
	5'-ACG UGA CAC GUU CGG AGA ATT-3'
Negative control FAM	5'-UUC UCC GAA CGU GUC ACG UTT-3'
	5'-ACG UGA CAC GUU CGG AGA ATT-3'
SOX7-Rat-86	5'-CCU CGU UGC UGG GCG CUU ATT-3'
	5'-UAA GCG CCC AGC AAC GAG GTT-3'
SOX7-Rat-288	5'-CCU GCA CAA CGC GGA GCU UTT-3'
	5'-AAG CUC CGC GUU GUG CAG GTT-3'
SOX7-Rat-1052	5'-GCA AUG AGU UUG ACC AGU ATT-3'
	5'-UAC UGG UCA AAC UCA UUG CTT-3'

mutant sites (mut) were amplified by PCR from cDNA of GH4C1 and inserted into the pMIR-REPORTER vector (Ambion; Austin, TX, USA). WT and mutant constructs were confirmed by sequencing. GH4C1 cells were seeded in a 24-well plate and cotransfected with either WT or mutant luciferase reporter plasmids containing the *Sox7*-3' UTR, pGL4.74 vector (Ambion), and equal amounts of mir-34a and miR-NC (GenePharma, Shanghai, China), using Lipofectamine 2000 according to the manufacturer's instructions. Luciferase activities were measured 24 hr after transfection using a dual luciferase assay kit (Promega, Madison, WI, USA). Experiments were performed in triplicate with three independent replicates.

### Statistical Analysis

All experiments were replicated three times. Results are reported as the means  $\pm$  SEM and were compared using the Student's *t* test in GraphPad PRISM software 5.0 (La Jolla, CA, USA). Differences were considered statistically significant at  $p < 0.05$ .

### SUPPLEMENTAL INFORMATION

Supplemental Information includes five tables and can be found with this article online at <https://doi.org/10.1016/j.omto.2018.07.001>.

### AUTHOR CONTRIBUTIONS

Z.Y. and T.Z. designed and performed the experiments and revised the manuscript. Z.Y. statistically analyzed the data and drafted the manuscript. Q.W. participated in sample collection and reviewed the experimental results. H.G. participated in the design of this study and helped to draft and revise the manuscript. All authors read and approved the final manuscript.

### ACKNOWLEDGMENTS

I would like to express my gratitude to all those who have helped me during the research working. I gratefully acknowledge the help of my mentor, Heng Gao. I do appreciate his patience, encouragement, and professional instructions.

The Jiangsu Provincial Natural Science Foundation of China (grant no. BK2011188) supported our work.

### REFERENCES

- Ezzat, S., Asa, S.L., Couldwell, W.T., Barr, C.E., Dodge, W.E., Vance, M.L., and McCutcheon, I.E. (2004). The prevalence of pituitary adenomas: a systematic review. *Cancer* 101, 613–619.
- Pichard, C., Gerber, S., Lalo, M., Kujas, M., Clemenceau, S., Ponvert, D., Bruckert, E., and Turpin, G. (2002). Pituitary carcinoma: report of an exceptional case and review of the literature. *J. Endocrinol. Invest.* 25, 65–72.
- Zhu, X., Wang, Y., Zhao, X., Jiang, C., Zhang, Q., Jiang, W., Wang, Y., Chen, H., Shou, X., Zhao, Y., et al. (2015). Incidence of pituitary apoplexy and its risk factors in Chinese people: a database study of patients with pituitary adenoma. *PLoS ONE* 10, e0139088.
- Cristina, C., Luque, G.M., Demarchi, G., Lopez Vicchi, F., Zubeldia-Brenner, L., Perez Millan, M.I., Perrone, S., Ornstein, A.M., Lacau-Mengido, I.M., Berner, S.L., and Becu-Villalobos, D. (2014). Angiogenesis in pituitary adenomas: human studies and new mutant mouse models. *Int. J. Endocrinol.* 2014, 608497.
- Hewedi, I.H., Osman, W.M., and El Mahdy, M.M. (2011). Differential expression of cyclin D1 in human pituitary tumors: relation to MIB-1 and p27/Kip1 labeling indices. *J. Egypt. Natl. Canc. Inst.* 23, 171–179.
- Stine, Z.E., Walton, Z.E., Altman, B.J., Hsieh, A.L., and Dang, C.V. (2015). MYC, metabolism, and cancer. *Cancer Discov.* 5, 1024–1039.
- Yang, E., and Korsmeyer, S.J. (1996). Molecular thanatopsis: a discourse on the BCL2 family and cell death. *Blood* 88, 386–401.
- Soini, Y., Pääkkö, P., and Lehto, V.P. (1998). Histopathological evaluation of apoptosis in cancer. *Am. J. Pathol.* 153, 1041–1053.
- Cebrián, M.J., Bauden, M., Andersson, R., Holdenrieder, S., and Ansari, D. (2016). Paradoxical role of HMGB1 in pancreatic cancer: tumor suppressor or tumor promoter? *Anticancer Res.* 36, 4381–4389.
- Richmond, J., Tuzova, M., Cruikshank, W., and Center, D. (2014). Regulation of cellular processes by interleukin-16 in homeostasis and cancer. *J. Cell. Physiol.* 229, 139–147.
- Stovall, D.B., Cao, P., and Sui, G. (2014). SOX7: from a developmental regulator to an emerging tumor suppressor. *Histol. Histopathol.* 29, 439–445.
- Ambros, V. (2004). The functions of animal microRNAs. *Nature* 431, 350–355.
- Garzon, R., Marcucci, G., and Croce, C.M. (2010). Targeting microRNAs in cancer: rationale, strategies and challenges. *Nat. Rev. Drug Discov.* 9, 775–789.
- Palumbo, T., Fauz, F.R., Azevedo, M., Xekouki, P., Iliopoulos, D., and Stratakis, C.A. (2013). Functional screen analysis reveals miR-26b and miR-128 as central regulators of pituitary somatotrophic tumor growth through activation of the PTEN-AKT pathway. *Oncogene* 32, 1651–1659.
- Bottoni, A., Piccin, D., Tagliati, F., Luchin, A., Zatelli, M.C., and degli Uberti, E.C. (2005). miR-15a and miR-16-1 down-regulation in pituitary adenomas. *J. Cell. Physiol.* 204, 280–285.
- Qian, Z.R., Asa, S.L., Siomi, H., Siomi, M.C., Yoshimoto, K., Yamada, S., Wang, E.L., Rahman, M.M., Inoue, H., Itakura, M., et al. (2009). Overexpression of HMGA2 relates to reduction of the let-7 and its relationship to clinicopathological features in pituitary adenomas. *Mod. Pathol.* 22, 431–441.
- Stilling, G., Sun, Z., Zhang, S., Jin, L., Righi, A., Kovács, G., Korbonits, M., Scheithauer, B.W., Kovacs, K., and Lloyd, R.V. (2010). MicroRNA expression in ACTH-producing pituitary tumors: up-regulation of microRNA-122 and -493 in pituitary carcinomas. *Endocrine* 38, 67–75.
- Peng, Y., Guo, J.J., Liu, Y.M., and Wu, X.L. (2014). MicroRNA-34A inhibits the growth, invasion and metastasis of gastric cancer by targeting PDGFR and MET expression. *Biosci. Rep.* 34, e00112.
- Ma, Z.L., Hou, P.P., Li, Y.L., Wang, D.T., Yuan, T.W., Wei, J.L., Zhao, B.T., Lou, J.T., Zhao, X.T., Jin, Y., and Jin, Y.X. (2015). MicroRNA-34a inhibits the proliferation and promotes the apoptosis of non-small cell lung cancer H1299 cell line by targeting TGF $\beta$ R2. *Tumour Biol.* 36, 2481–2490.
- Li, S.Z., Hu, Y.Y., Zhao, J., Zhao, Y.B., Sun, J.D., Yang, Y.F., Ji, C.C., Liu, Z.B., Cao, W.D., Qu, Y., et al. (2014). MicroRNA-34a induces apoptosis in the human glioma cell line, A172, through enhanced ROS production and NOX2 expression. *Biochem. Biophys. Res. Commun.* 444, 6–12.

21. Li, G., Yao, L., Zhang, J., Li, X., Dang, S., Zeng, K., Zhou, Y., and Gao, F. (2016). Tumor-suppressive microRNA-34a inhibits breast cancer cell migration and invasion via targeting oncogenic TPD52. *Tumour Biol.* 37, 7481–7491.
22. Yu, G., Xu, K., Xu, S., Zhang, X., Huang, Q., and Lang, B. (2015). [MicroRNA-34a regulates cell cycle by targeting CD44 in human bladder carcinoma cells]. *Nan Fang Yi Ke Da Xue Xue Bao* 35, 935–940.
23. Yu, X., Zhang, L., Wen, G., Zhao, H., Luong, L.A., Chen, Q., Huang, Y., Zhu, J., Ye, S., Xu, Q., et al. (2015). Upregulated sirtuin 1 by miRNA-34a is required for smooth muscle cell differentiation from pluripotent stem cells. *Cell Death Differ.* 22, 1170–1180.
24. Zhang, D., Zhou, J., and Dong, M. (2014). Dysregulation of microRNA-34a expression in colorectal cancer inhibits the phosphorylation of FAK via VEGF. *Dig. Dis. Sci.* 59, 958–967.
25. Yu, G., Yao, W., Xiao, W., Li, H., Xu, H., and Lang, B. (2014). MicroRNA-34a functions as an anti-metastatic microRNA and suppresses angiogenesis in bladder cancer by directly targeting CD44. *J. Exp. Clin. Cancer Res.* 33, 779.
26. Qiao, P., Li, G., Bi, W., Yang, L., Yao, L., and Wu, D. (2015). microRNA-34a inhibits epithelial mesenchymal transition in human cholangiocarcinoma by targeting Smad4 through transforming growth factor-beta/Smad pathway. *BMC Cancer* 15, 469.
27. Liu, K., Huang, J., Xie, M., Yu, Y., Zhu, S., Kang, R., Cao, L., Tang, D., and Duan, X. (2014). MIR34A regulates autophagy and apoptosis by targeting HMGB1 in the retinoblastoma cell. *Autophagy* 10, 442–452.
28. Li, X.Y., Wen, J.Y., Jia, C.C., Wang, T.T., Li, X., Dong, M., Lin, Q.U., Chen, Z.H., Ma, X.K., Wei, L.L., et al. (2015). MicroRNA-34a-5p enhances sensitivity to chemotherapy by targeting AXL in hepatocellular carcinoma MHCC-97L cells. *Oncol. Lett.* 10, 2691–2698.
29. Li, X.J., Ren, Z.J., and Tang, J.H. (2014). MicroRNA-34a: a potential therapeutic target in human cancer. *Cell Death Dis.* 5, e1327.
30. Yamakuchi, M., and Lowenstein, C.J. (2009). MiR-34, SIRT1 and p53: the feedback loop. *Cell Cycle* 8, 712–715.
31. Li, B., Ge, Z., Song, S., Zhang, S., Yan, H., Huang, B., and Zhang, Y. (2012). Decreased expression of SOX7 is correlated with poor prognosis in lung adenocarcinoma patients. *Pathol. Oncol. Res.* 18, 1039–1045.
32. Stovall, D.B., Wan, M., Miller, L.D., Cao, P., Maglic, D., Zhang, Q., Stampfer, M.R., Liu, W., Xu, J., and Sui, G. (2013). The regulation of SOX7 and its tumor suppressive role in breast cancer. *Am. J. Pathol.* 183, 1645–1653.
33. Cuvertino, S., Filicetto, G., Masarekar, A., Saha, V., Lacaud, G., and Kouskoff, V. (2016). SOX7 promotes the maintenance and proliferation of B cell precursor acute lymphoblastic cells. *Oncotarget* 8, 64974–64983.
34. Katoh, M. (2002). Expression of human SOX7 in normal tissues and tumors. *Int. J. Mol. Med.* 9, 363–368.
35. Futaki, S., Hayashi, Y., Emoto, T., Weber, C.N., and Sekiguchi, K. (2004). Sox7 plays crucial roles in parietal endoderm differentiation in F9 embryonal carcinoma cells through regulating Gata-4 and Gata-6 expression. *Mol. Cell. Biol.* 24, 10492–10503.
36. Kim, I.K., Kim, K., Lee, E., Oh, D.S., Park, C.S., Park, S., Yang, J.M., Kim, J.H., Kim, H.S., Shima, D.T., et al. (2018). Sox7 promotes high-grade glioma by increasing VEGFR2-mediated vascular abnormality. *J. Exp. Med.* 215, 963–983.
37. Yang, Y., Andersson, P., Hosaka, K., Zhang, Y., Cao, R., Iwamoto, H., Yang, X., Nakamura, M., Wang, J., Zhuang, R., et al. (2016). The PDGF-BB-SOX7 axis-modulated IL-33 in pericytes and stromal cells promotes metastasis through tumour-associated macrophages. *Nat. Commun.* 7, 11385.